

Estimation of underwater visibility in coastal and inland waters using remote sensing data

Anuj Kulshreshtha  · Palanisamy Shanmugam

Received: 16 August 2016 / Accepted: 21 March 2017 / Published online: 30 March 2017
© Springer International Publishing Switzerland 2017

Abstract An optical method is developed to estimate water transparency (or underwater visibility) in terms of Secchi depth (Z_{sd}), which follows the remote sensing and contrast transmittance theory. The major factors governing the variation in Z_{sd} , namely, turbidity and length attenuation coefficient ($1/(c + K_d)$, c = beam attenuation coefficient; K_d = diffuse attenuation coefficient at 531 nm), are obtained based on band rationing techniques. It was found that the band ratio of remote sensing reflectance (expressed as $(R_{rs}(443) + R_{rs}(490))/(R_{rs}(555) + R_{rs}(670))$) contains essential information about the water column optical properties and thereby positively correlates to turbidity. The beam attenuation coefficient (c) at 531 nm is obtained by a linear relationship with turbidity. To derive the vertical diffuse attenuation coefficient (K_d) at 531 nm, $K_d(490)$ is estimated as a function of reflectance ratio ($R_{rs}(670)/R_{rs}(490)$), which provides the bio-optical link between chlorophyll concentration and $K_d(531)$. The present algorithm was applied to MODIS-Aqua images, and the results were evaluated by matchup comparisons between the remotely estimated Z_{sd} and in situ Z_{sd} in coastal waters off Point Calimere and its adjoining regions on the southeast coast of India. The results showed the pattern of

increasing Z_{sd} from shallow turbid waters to deep clear waters. The statistical evaluation of the results showed that the percent mean relative error between the MODIS-Aqua-derived Z_{sd} and in situ Z_{sd} values was within $\pm 25\%$. A close agreement achieved in spatial contours of MODIS-Aqua-derived Z_{sd} and in situ Z_{sd} for the month of January 2014 and August 2013 promises the model capability to yield accurate estimates of Z_{sd} in coastal, estuarine, and inland waters. The spatial contours have been included to provide the best data visualization of the measured, modeled (in situ), and satellite-derived Z_{sd} products. The modeled and satellite-derived Z_{sd} values were compared with measurement data which yielded $RMSE = 0.079$, $MRE = -0.016$, and $R^2 = 0.95$ for the modeled Z_{sd} and $RMSE = 0.075$, $MRE = 0.020$, and $R^2 = 0.95$ for the satellite-derived Z_{sd} products.

Keywords Secchi disk depth · Turbidity · Remote sensing reflectance · Coastal waters · Chlorophyll concentration · Total suspended sediments

Abbreviations

TSI	Trophic state index
SeaWiFS	Sea-Viewing Wide Field-of-View Sensor
DN	Digital number
TM	Thematic mapper
GLMs	Generalized linear models
GAMs	Generalized additive models
AC-S	Absorption and attenuation sensors
BB9	Backscattering sensors

A. Kulshreshtha · P. Shanmugam (✉)
Department of Ocean Engineering, Ocean Optics and Imaging
Laboratory, Indian Institute of Technology Madras,
Chennai 600036, India
e-mail: pshanmugam@iitm.ac.in

A. Kulshreshtha
e-mail: anujk3dec@gmail.com

IOPs	Inherent optical properties
ECO	Environmental characterization optics
FLNTU	Turbidity and fluorescence chlorophyll sensors
TSS	Total suspended sediment
ABI	Algal bloom index
RMSE	Root mean square error
MRE	Mean root error
NTU	Nephelometric turbidity unit
SAV	Submerged aquatic vegetation
CDOM	Colored dissolved organic matter
$a(\lambda)$	Absorption coefficient
$a-a_w$	Particulate absorption coefficient
$b_b(\lambda)$	Backscattering coefficient
$c-c_w$	Particulate attenuation coefficient
Z_{sd}	Secchi depth
K_d	Vertical diffuse attenuation coefficient
$K_{d,PAR}$	Vertical diffuse attenuation coefficient for photosynthetically active radiation
$c(\lambda)$	Beam attenuation coefficient
$b(\lambda)$	Scattering coefficient
$1/(c + K_d)$	Length attenuation coefficient
Γ	Coupling coefficient
$E_{d,\lambda}$	Spectral downwelling irradiance
R_{rs}	Remote sensing reflectance
L_t	Total radiances
nL_w	Normalized water leaving radiance
N	Number of data-points
R^2	Correlation coefficient

Introduction

The water quality mapping and its assessment on a regional-global scale has been a field of interest to environmentalists, marine scientists, and oceanographers over the decades (Suresh et al. 2006). One of the standard parameters that provide the primary information about the optical characteristics of the water column and water transparency is the Secchi depth (denoted by Z_{sd}). Due to ease of measurement, it is widely used as a tool to assess the quality of regional and global water bodies (Holmes 1970; Steel and Neuhausser 2002; Trees et al. 2005; Berkman and Canova 2007; Balali et al. 2013). The Z_{sd} parameter has assisted to develop the trophic state index (TSI) which can be used to assess the eutrophication status of lakes and inland water bodies. The TSI has been recognized as an important

predictive tool to monitor the biological conditions (algal biomass or nutrient concentration) of lakes and inland waters (Carlson 1977). The water transparency parameter and prediction of diver's visibility have major implications in port and harbor security and are quite instrumental to recreational and commercial diving industries (Trees et al. 2005).

The in situ measurements of optical properties to estimate the water transparency parameter are a time-consuming and cumbersome activity on water bodies that cover a large aerial extent. To overcome this limitation, several algorithms have been developed for remote sensing of Z_{sd} in regional water bodies. Over the last three decades, remote sensing has played a pivotal role in providing synoptic information about the water constituents and their variations in marine and inland waters. The significant advancement in the field of remote sensing and its application has potentially enhanced water management and monitoring activities (Chen et al. 2007b; Moreno 2013).

Several empirical and semi-empirical algorithms have been developed to estimate Z_{sd} from remote sensing data. Many of these algorithms deviate from the concept of contrast transmittance theory yielding significant errors in Z_{sd} products.

The study conducted in the sub-alpine lake Iseo (Italy) region used Landsat TM data to map Z_{sd} and estimate the euphotic depth (Giardino et al. 2001). This study showed that the blue-green band ratio provides reliable results in inland waters despite that the regression relationships lacked consistency and highly relied on water quality sampling during satellite passages. The algorithm mainly depended on the correlation between atmospherically corrected reflectance values to predict the trend of Z_{sd} in the lake water.

$$SD = 8.01 \times (\rho_{TM1}/\rho_{TM2}) - 8.27 \quad (1)$$

where "SD" refers to Secchi depth and ρ_{TM1}/ρ_{TM2} represents the ratio of atmospherically corrected reflectance values at bands TM1 and TM2.

In another study carried out in the Gulf of Finland and Archipelago Sea, a multivariate algorithm was derived by combining the digital number (DN) values of Landsat 7 thematic mapper (TM) bands (optical) and $ERS-2$ SAR (microwave) remote sensing data (Zhang et al. 2003). The formulation consisted of regression coefficients obtained on comparison of the measured

sea-truth data with satellite observed data. The expression takes the form

$$SDD_{TM} = A_0 + \sum_{i=1}^7 A_i(TM_i) \tag{2}$$

$$SDD_{TM/SAR} = B_0 + \sum_{i=1}^7 B_i(TM_i) + B(SAR) \tag{3}$$

where ‘‘SDD’’ = Secchi depth and $A_0, A_i, B_0, B_i,$ and B = derived regression coefficients. The neural network algorithm was also applied on the same data set to derive Z_{sd} products. This study suggested that the multivariate algorithms and neural network technique can be an effective way to estimate Z_{sd} in coastal waters.

Similarly, Suresh et al. (2006) derived an empirical formula that estimates Z_{sd} values as a function of the remote sensing reflectance (R_{rs}) band ratio ($R_{rs}(490)/R_{rs}(555)$) through

$$Z_{sd} = A + B \left(\frac{R_{rs}(490)}{R_{rs}(555)} \right) \tag{4}$$

where $A = 2.27212$ and $B = 7.239$.

This method was tested on Sea-Viewing Wide Field-of-View Sensor (SeaWiFS) and IRS P-4 OCM data in the Arabian Sea off Gujarat and west coast of India with a limited in situ matchup data set.

In another study, the satellite maps of Z_{sd} between the periods 2003 and 2012 were used to assess the eutrophication status for the region of the Baltic Sea (Stock 2015). The study was focused on the generalized linear models (GLMs) and generalized additive models (GAMs) to predict Z_{sd} on a regional scale. The satellite-based Z_{sd} algorithm consists of a regionally calibrated linear model and employed R_{rs} ratio of 488 to 645 nm, which is given by

$$\ln(Z_{sd}^{-1}) = 1.3405 + \ln \left(\frac{R_{rs}(488)}{R_{rs}(645)} \right) - 0.4343 \tag{5}$$

The in situ Z_{sd} was also empirically correlated to satellite $K_d(490)$ with an aim to study and monitor water quality in estuarine waters of Tampa Bay (Chen et al. 2007b). A two-step algorithm was formulated and employed—i.e., estimating $K_d(490)$ through a semi-analytical algorithm and deriving Z_{sd} from an empirical formula as a function of $K_d(490)$. This study further demonstrated various

spatial-temporal characteristics and time series trends of Z_{sd} derived from satellite data. The empirical relationship to derive Z_{sd} is given by

$$SDD = 1.04 \times K_d(490)^{-0.82} \tag{6}$$

A mechanistic model has been developed recently to estimate the underwater visibility in marine and inland waters (Lee et al. 2015). This model takes the form

$$Z_{sd} = \frac{1}{2.5 \text{Min}(K_d(443, 488, 532, 555, 665))} \ln \left(\frac{|0.14 - R_{rs}^{pc}|}{C_t^r} \right) \tag{7}$$

The model depends on the complex technique of measuring the threshold contrast of the sighting range of the white disk to estimate Z_{sd} , and the correlation of coupling coefficient (I) to in-water inherent optical properties ($IOPs$) which forms the integral component of the contrast transmittance theory in estimating Z_{sd} (Tyler 1968; Davies-Colley 1988; Lee et al. 2015).

It can be inferred that the above Eqs. (1)–(7) either ignored the concept of contrast transmittance theory entirely or failed to address the important role of the coupling coefficient, which necessitated the development of a new algorithm that can establish the importance of the contrast transmittance theory and coupling coefficient to accurately derive Z_{sd} from satellite data for improved water quality monitoring applications.

The above studies highly rely on the empirical and semi-empirical relationships obtained from the band ratio techniques to capture the Z_{sd} variation in the water column. Moreover, these studies revealed that the existing satellite-derived Z_{sd} algorithms do not adopt the well-recognized principle concept of the contrast transmittance theory and solely depended on either optical properties or the R_{rs} band ratio. Therefore, these algorithms did not focus to explain the physical significance of the coupling coefficient which forms the integral parameter of the contrast transmittance theory. Such algorithms lacked the crucial step to retrieve the coupling coefficient based on the satellite remote sensing technique. Bearing in mind, a satellite-derived Z_{sd} algorithm is developed in the present study within the framework of the contrast transmittance theory that well accounts for the influence of the length attenuation coefficient ($1/(c + K_d)$) and coupling coefficient. In contrast to existing algorithms, the proposed method reveals effective and simple steps to estimate the coupling coefficient following the principles of ocean color remote sensing. It can be further implied that the present study

intends to lay emphasis that the integral component of the contrast transmittance theory (especially the coupling coefficient) must not be ignored. Furthermore, the satellite-based Z_{sd} for coastal, estuarine, and inland water bodies can be estimated following the principles of the contrast transmittance theory provided the algorithm aptly accounts for the method to estimate the coupling coefficient. The present work aims to demonstrate that the accurate estimation of Z_{sd} can be achieved using the remote sensing data, following the Z_{sd} algorithm proposed by Kulshreshtha and Shanmugam (2015), which takes the advantages of using the contrast transmittance theory, coupling coefficient, and optical parameters (turbidity, $c(531)$, and $K_d(531)$) to predict Z_{sd} for water quality assessment and monitoring programs.

Materials and methods

In situ data The absorption coefficient ($a(\lambda)$) and attenuation coefficient ($c(\lambda)$) were measured on-board using absorption and attenuation sensors (AC-S) (WET Labs Inc.) in the spectral range of 400–700 nm, whereas the backscattering coefficient ($b_b(\lambda)$) was measured using a backscattering sensor (BB9) (WET Labs Inc.) at nine wavelengths (namely, 412, 440, 488, 512, 530, 565, 650, 676, and 715 nm). The temperature and salinity correction was applied to measured AC-S data, and thereafter, scattering correction was performed on salinity-temperature-corrected absorption data to determine the particulate absorption coefficient (a_{-a_w}) and particulate attenuation coefficient (c_{-c_w}) (Pegau and Zaneveld 1993; Zaneveld and Kitchen 1994; Pegau et al. 1997). Here, the subscript “w” represents pure water components respectively for both the absorption and attenuation coefficients. Subsequently, the value of c_w was added to the measured particulate attenuation coefficient (c_{-c_w}) to obtain the total beam attenuation coefficient (c) at desired wavelengths (Pope and Fry 1997).

Moreover, three hyperspectral radiometers (TriOS RAMSES radiometers) were employed for underwater radiometric profiling measurements. These radiometric quantities (upwelling radiance, downwelling irradiance, and upwelling irradiance) recorded in the system were then exported to deck PC and processed. The immersion factors (wavelength-dependent correction factors) were also applied to radiance data owing to the fact that the radiance sensor was immersed (Ohde and Siegel 2003).

Apart from these underwater radiometric quantities, above-water radiometers were also employed to measure sky radiance, total water-leaving radiance, and downwelling irradiance. The total water-leaving radiance was then determined based on the protocol by Mobley (1999). The underwater radiometric quantities and IOPs were measured at various discrete depths and wavelengths. These parameters were interpolated to common depth and wavelength so as to ensure the consistency of the input data for the model. The Z_{sd} measurement was carried out using a standard Secchi disk, with a circular diameter of 20 cm. The disk had black and white quadrants painted on its surface which was lowered vertically using a rope tied to the center of the disk. The vertical rope was graduated at every 0.2 m to meticulously record the depth at which the disk disappeared and re-appeared. The Z_{sd} measurements were carried out away from the ship or boat to avoid any shadowing effect following the standard protocols (Smith 2001).

In the present study, two data sets, namely, NASA bio-Optical Marine Algorithm Data set (NOMAD) and Indian (measured off Point Calimere) data set, were used to develop the algorithm. The NOMAD data were downloaded from the IOCCG website (http://www.ioccg.org/data_ioccg.html) which consist of in situ data collected between the periods 1996 and 2006. The NOMAD data were extracted from the SEABASS database that included the vertical diffuse attenuation coefficient $K_d(490)$, $R_{rs}(490)$, $R_{rs}(670)$, and chlorophyll concentration. The selected NOMAD data provided the desired reliability to develop the intermediate model for deriving K_d . However, it has been recognized that the NOMAD data do not contain turbidity and “c”; therefore, these variables were obtained solely from the Indian data set. The Indian data set consists of in situ data collected from clear and turbid coastal waters off Point Calimere (sampling stations marked inside rectangle) and Chennai (sampling stations marked inside oval) within the region of Bay of Bengal during the months of May 2012, August 2012, August 2013, and January 2014 (Fig. 1a). The Point Calimere region is located in the southeast part of India bounded by the latitude and longitude of 10.2878° N and 79.8651° E. The study region, located near Vadaranniyam coastal wetlands, is largely influenced by sediment runoff discharged by seasonal river flows (e.g., Cauvery river), while the human interferences like aquaculture and salt panning activities in the western part of Point

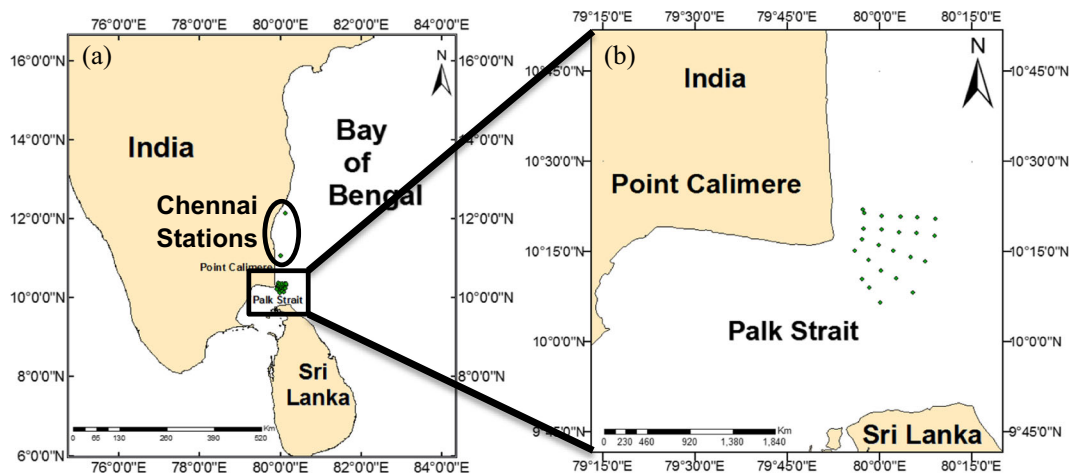


Fig. 1 The geographical map illustrating the sampling stations for the study region. **a** Sampling stations located at Point Calimere (marked inside *rectangle*) and Chennai (marked inside *oval*). **b**

Clear and turbid coastal water sampling stations established on each of the five transects off Point Calimere

Calimere have resulted in sediment accretion. The geomorphological features of the study region essentially include numerous mudflats and creeks (Mullipallam and Serattalaikkadu creeks) whose areal extent has undergone a marginal decrease. The low-energy streams like Marakkakoraiyar, Valavnar, Koraiyar, and Kilaittangi together with tides, currents, and waves have resulted in dominance of suspended sediments in the shallow region of Palk Bay and Point Calimere (Selvaraj et al. 2005). It can be implied that the study region experiences dynamic changes owing to the fluctuations in river discharge and sediment loading caused due to certain coastal processes and the increased human activities.

A total of 24 sampling stations were established on five different transects, with stations located adjacently on each transect, covering the relatively clear to highly turbid coastal waters (Fig. 1b). The in situ data collected on-board for the month of August 2013 and January 2014 was used to develop the model, while the validation was carried out with the in situ data collected during the month of May 2012 and August 2012. The cruise program prevailed for about 6 days (or a week) during each of these months. Therefore, it must be noted that in situ data were collected from 24 sampling stations in duration of a week with approximately four sampling stations visited each day of the cruise program. For validating the proposed algorithm, the in situ samples were matched to a satellite within a 2-h window coincident with satellite overpass in order

to ensure a minimum discrepancy. The underwater optical instruments were essentially the depth profilers which recorded the in situ data all along the depth of the water column at each sampling stations. The intermediate parametrizations and independent validation were carried out based on the principles of the remote sensing technique following a careful selection of in situ data. K_d was calculated from spectral downwelling irradiance ($E_d(\lambda, z)$) measured just below the water surface and at a depth of 1 m, which may be regarded as K_d at a depth of 1 m (further details in Simon and Shanmugam 2013; Simon and Shanmugam 2016). Moreover, the average value of turbidity and chlorophyll concentration (depth averaged within 1 m of the water column) was used to develop the bio-optical relationships. A similar approach was adopted for independent data sets which demonstrated a robust independent validation performed between the modeled and satellite-derived Z_{sd} values. The algorithm for turbidity was developed using the Indian data ($N = 59$) collected during the month of August 2013 and January 2014. The data set consisted of in situ R_{rs} and turbidity (expressed in terms of NTU). The c at 531 nm is parameterized in terms of turbidity (NTU) using the Indian data set ($N = 416$). The data reflected a large range of variation in optical properties of waters commonly found within coastal environments. Using the Indian data set, a total of 59 data were chosen to develop a model for turbidity and 416 data were used to model c . An independent

data set of 32 samples was used to validate the modeled turbidity values. Similarly, an independent data set of 69 samples was used to validate the modeled c . These independent data sets were chosen from the Indian in situ database. A model estimating $K_d(531)$ was developed based on the NOMAD ($N = 827$) and Indian ($N = 72$) data. An independent validation of the modeled $K_d(531)$ was performed using the Indian data set ($N = 61$).

The turbidity data were collected by an environmental characterization optics (ECO) turbidity and fluorescence chlorophyll sensors (FLNTU) sensor. An ECO FLNTU sensor is a dedicated instrument designed to measure in situ turbidity and chlorophyll-a simultaneously which was procured from WET Labs (USA). It records turbidity in nephelometric turbidity units (NTUs) based on scattering measurements at 700 nm and chlorophyll concentration in terms of micrograms per liter by measuring the fluorescence at the excitation/emission wavelengths of 470/695 nm (WETLabs 2010).

In both clear and turbid waters, turbidity varied from 0.05 to 20 NTU and chlorophyll concentration varied from 0.04 to 18.5 $\mu\text{g l}^{-1}$. The total suspended sediment (TSS in mg l^{-1}) was calculated from measured turbidity based on a power relationship developed by Ellison et al. (2010).

Satellite data Several MODIS-Aqua data (level 1A, local area coverage, pixel resolution of about 1.1×1.1 km at nadir) covering the study area were obtained from NASA's Goddard Space Flight Space Center (<http://oceancolor.gsfc.nasa.gov/>). These MODIS images were selected because they were cloud free and concurrently matched with the in situ data. The MODIS-Aqua images were processed using SeaDAS 7.2 software to provide calibrated and scaled level 1B products yielding the total radiances (L_t) at the top of the atmosphere. The level 1B data were atmospherically corrected using the standard Rayleigh correction scheme (embedded in SeaDAS 7.2) and a new aerosol correction scheme (Singh and Shanmugam 2014). Subsequently, the normalized water leaving radiance " nL_w " and R_{rs} were obtained as key inputs for deriving the intermediate (e.g., turbidity from this study and chlorophyll from Shanmugam 2011) and end products. In the present study, the ABI_Chlor-a algorithm (Shanmugam 2011) was used to retrieve the

chlorophyll-a (Chl-a) concentration from satellite data. The algorithm uses the ratios of nL_w at three bands (i.e., 443, 490, and 555 nm) of the visible spectrum, in conjunction with algal bloom index (ABI) formula to accurately estimate Chl-a in coastal and oceanic waters. This method of retrieving the Chl-a from satellite data is composed of two integral steps where the preliminary step involves the calculation of ABI which is given by

$$X = \text{ABI} = 10 \left[\left(\frac{nL_w(490)}{nL_w(555)} \right) - \left(\frac{nL_w(490)}{\alpha} \right) \right] / \left[\left(\frac{nL_w(490)}{nL_w(555)} \right) + \left(\frac{nL_w(443)}{\alpha} \right) \right] \quad (8)$$

where the value of " α " is assumed to be unity. Thereafter, a variable factor, X' , is calculated to reduce the uncertainties in the retrieved Chl-a given by

$$X' = \left(\frac{(nL_w(443) \times nL_w(490) / nL_w(555))^2}{(\lambda_{490} - \lambda_{443})} \right) \quad (9)$$

The second step requires initial estimation of chlorophyll-a concentration ε_{Chl-a} which is expressed as a power law function of the multiplication factor " \mathbf{X} ". is obtained simply as the product of ABI and the variable factor X' given by

$$\mathbf{X} = X \times X' \quad (10)$$

And the correlation between ε_{Chl-a} and \mathbf{X} is expressed as

$$\varepsilon_{Chl-a} = 0.1403 \times (\mathbf{X})^{(-0.572)} \quad (11)$$

Finally, the capability of ε_{Chl-a} to estimate Chl-a over a wide variety of water types is improved by fine tuning it, which yields the final expression for Chl-a as

$$\text{ABI_Chl-a} = 125 \frac{\varepsilon_{chl-a}^{1.056}}{(126.69 + \varepsilon_{chl-a}^{1.056})^{0.96}} \quad (12)$$

For validation, a number of matchup pairs from in situ and MODIS-Aqua data were collected for the months of January 2014 and August 2013.

Performance assessment

The performance of the present algorithm was assessed based on some standard statistical parameters calculated between the satellite-derived Z_{sd} values and measured (in situ) Z_{sd} values. These statistical measures included root mean square error (RMSE), mean relative error

(MRE), bias, slope, intercept, and correlation coefficient (R^2). The RMSE and MRE values were calculated by the respective matrices given by Eqs. (13) and (14), respectively.

$$RMSE = \left[\frac{\sum_{i=1}^n (\log Z_{sd}^{satellite} - \log Z_{sd}^{in situ})^2}{N-2} \right]^{1/2} \tag{13}$$

$$MRE = \sum_{i=1}^n \left(\frac{\log Z_{sd}^{satellite} - \log Z_{sd}^{in situ}}{\log Z_{sd}^{in situ}} \right) \times 100 \tag{14}$$

These statistical measures were useful to assess the accuracy of the derived products from satellite data.

Results

Secchi depth algorithm The underwater vertical visibility parameter, defined in terms of Z_{sd} , essentially depends on two major factors, namely, the coupling coefficient and the length attenuation coefficient, and hence obeys the principle of the contrast transmittance theory (Tyler 1968; Preisendorfer 1986; Davies-Colley 1988; Doron et al. 2007; Hou et al. 2007). The well-recognized relationship to estimate the water transparency in terms of Z_{sd} is given by

$$Z_{sd} \propto \frac{1}{c + K_d} \text{ or } Z_{sd} = \frac{\Gamma}{c + K_d} \tag{15}$$

where $(1 / (c + K_d)) =$ length attenuation coefficient.

$\Gamma =$ Coupling coefficient

The inverse of the additive sum of c and K_d as defined by the length attenuation coefficient is expressed as $(1 / (c + K_d))$ in a unit of m . The c is a measure of the amount of light intensity lost as it penetrates through the water column, which is expressed as the sum of the absorption coefficient (a) and scattering coefficient (b)

$$c(\lambda) = a(\lambda) + b(\lambda) \tag{16}$$

K_d is expressed as the logarithmic rate at which extinction of light intensity occurs as it penetrates through the water column and is given by

$$K_{d,\lambda}(z_2 - z_1) = \frac{-1}{z_2 - z_1} \ln \left(\frac{E_{d,\lambda}(z_2)}{E_{d,\lambda}(z_1)} \right) \tag{17}$$

where $E_{d,\lambda}(z_1) =$ spectral downwelling irradiance at depth z_1

$E_{d,\lambda}(z_2) =$ spectral downwelling irradiance at depth z_2 .

Equation (15) summarizes the contrast transmittance theory which states that Z_{sd} or the depth at which an object disappears, when lowered into the water column of a particular depth, is directly proportional to the length attenuation coefficient and is governed by an undetermined coupling coefficient. The value of the coupling coefficient varies from 5.9 to 10.1, while it is considerably higher in medium characterized by strong scattering (Hou et al. 2007). This imposes a greater challenge and constrains in predicting accurately the value of the coupling coefficient and hence the variation in Z_{sd} for optically complex turbid waters.

In order to overcome this problem, several studies reported Z_{sd} algorithms that solely relied on the R_{rs} band ratios or the inverse function of K_d or c or the sum of these two parameters. Such algorithms break down in turbid coastal waters due to twofold problems: they do not follow the equation of the contrast transmittance theory and they do not address how the varying value of the coupling coefficient can be predicted for various water types to estimate Z_{sd} values. This suggests that the Z_{sd} products derived from these algorithms may be biased with errors and consequently their applicability is questionable for improved water quality monitoring programs.

In the present work, these two issues are addressed based on our previous work (Kulshreshtha and Shanmugam 2015) and a new approach to predict the varying value of the coupling coefficient, and hence, the variation in Z_{sd} is proposed for satellite applications. The accurate estimates of Z_{sd} can now be achieved through

$$Z_{sd} = \frac{4.6 + (0.7585 \times \text{Turbidity})}{c(531) + K_d(531)} \tag{18}$$

using the three key parameters such as turbidity, c , and K_d . c and K_d are estimated at 531 nm owing to the fact that the penetration of the light occurs maximum in green wavelengths of the visible spectrum for both turbid and relatively clear waters. Moreover, most of the underwater imaging systems either active or passive operate in this spectral region. The underwater imaging systems include the unmanned remotely controlled or robotic underwater systems that use an imaging technique to map the type of submerged aquatic vegetation (SAV), to explore the sunken object or bottom debris, and to characterize the sea bed (Siegel and Dickey 1988;

Levin et al. 2013). The underwater visibility equation (Eq. (18)) strictly follows the contrast transmittance theory and, therefore, is considered an integral step to develop the satellite-based Z_{sd} algorithm. The feasibility of Eq. (18) to accurately estimate Z_{sd} is examined based on the in situ optical properties, and its results are presented in a later section. Figure 2 shows the schematic of this approach to estimate Z_{sd} from satellite data. The implementation of the proposed algorithm requires a step-wise derivation of input parameters, namely, turbidity, $c(531)$, and $K_d(531)$. Considering this sequence, step 1 employs the R_{rs} band ratio at 443, 490, 555, and 670 nm to derive the turbidity relationship. Models for $c(531)$ and $K_d(531)$ are then derived from the turbidity and $Chl-a$ parameters. The $K_d(531)$ relationship is based on the power law function relating $K_d(490)$ to $Chl-a$. The final step uses these parameters in the proposed formula to estimate Z_{sd} in inland and marine waters.

The turbidity, the important parameter governing the variation in the coupling coefficient, was derived as a function of R_{rs} , invoking the conventional band ratio technique (Chauhan et al. 2005; Chen et al. 2007a; Ouillon et al. 2008; Akbar et al. 2014; Tiwari and Shanmugam 2014; Nasiha and Shanmugam 2015). To achieve the desired model of turbidity, various combinations of the band ratio were systematically tested to derive accurate estimates of turbidity in both coastal and offshore waters. This study led to a model that shows a positive correlation between the light reflected in the bands (namely, 443, 490, 555, and 670 nm) and the optical property of the water column. It was found that the reflectance band ratio involving four bands in the blue-green-red region ($R_{rs}(443) + R_{rs}(490)/(R_{rs}(555) + R_{rs}(670))$) is tightly correlated to turbidity of various water types ($R^2 = 0.89$; Fig. 3a).

$$\text{Turbidity} = 7.6028 \times \left(\frac{R_{rs}(443) + R_{rs}(490)}{R_{rs}(555) + R_{rs}(670)} \right)^{-4.978} \quad (19)$$

The validation showed that the four-band algorithm yielded a considerably low error ($RMSE = 0.17$) and closely predicted the measured turbidity with $R^2 = 0.91$ ($N = 32$; Fig. 3b).

The length attenuation coefficient, another important optical property used in Eq. (18), is estimated by a two-step algorithm. c is derived as a linear function of turbidity, followed by the derivation of K_d . It was found that turbidity positively correlates to c following a linear

relationship with a slope of 1.0049 and $R^2 \sim 0.89$ (Eq. (20); Fig. 4a).

$$c(531) = 1.0049 \times \text{Turbidity} \quad (20)$$

The validation result revealed that this empirical formula gives estimates of $c(531)$ closely agreeing with the measured data ($R^2 = 0.97$; $RMSE = 0.16$; $N = 69$) (Fig. 4b). $K_d(531)$ is estimated through an intermediate parameter (i.e., $K_d(490)$), which can be easily determined using the band ratio of R_{rs} ($R_{rs}(670)/R_{rs}(490)$) (Eq. (21) and Fig. 5a) (Tiwari and Shanmugam 2014). The $R_{rs}(670)/R_{rs}(490)$ is linearly correlated to $K_d(490)$ ($R^2 = 0.92$).

$$K_d(490) = 1.2461 \times \left(\frac{R_{rs}(670)}{R_{rs}(490)^{rs}} \right) \quad (21)$$

Equation (21) when compared with that of Tiwari and Shanmugam (2014) showed that these two equations differ significantly in terms of slope and intercept and this difference could arise from different data sets used to derive the $K_d(490)$ relationships. The present study used a combined data set of NOMAD and Indian data, whereas Tiwari and Shanmugam (2014) relied on the IOCCG data set for their study. $K_d(490)$ provides the crucial bio-optical link between chlorophyll concentration and $K_d(531)$. The selection of $K_d(490)$ to derive $K_d(531)$ is based on the physics that the variation in the spectral slope of K_d from the blue-to-green region of the visible spectrum is mainly attributed to the variation in chlorophyll concentration. At shorter wavelengths in the blue-green band, the slope of $K_d(490)$ to $K_d(531)$ increases with the increase in chlorophyll concentration. However, such spectral behavior of K_d is not observed at longer wavelengths owing to the very high absorption by water (Berwald et al. 1998; Tiwari and Shanmugam 2014). Thus, the inverse slope-based power function best demonstrates the bio-optical relationship between chlorophyll concentration and the ratio of K_d at 531 nm to K_d at 490 nm (Eqs. (22) and (23)) (Fig. 5b).

$$K_d(531) = m \times K_d(490) \quad (22)$$

$$\text{where } m = 1.0776 \times Chl^{-0.176} \quad (23)$$

where “ m ” is the slope that governs the magnitude of $K_d(490)$, which depends on the chlorophyll concentration and varies in different waters. Thus, the

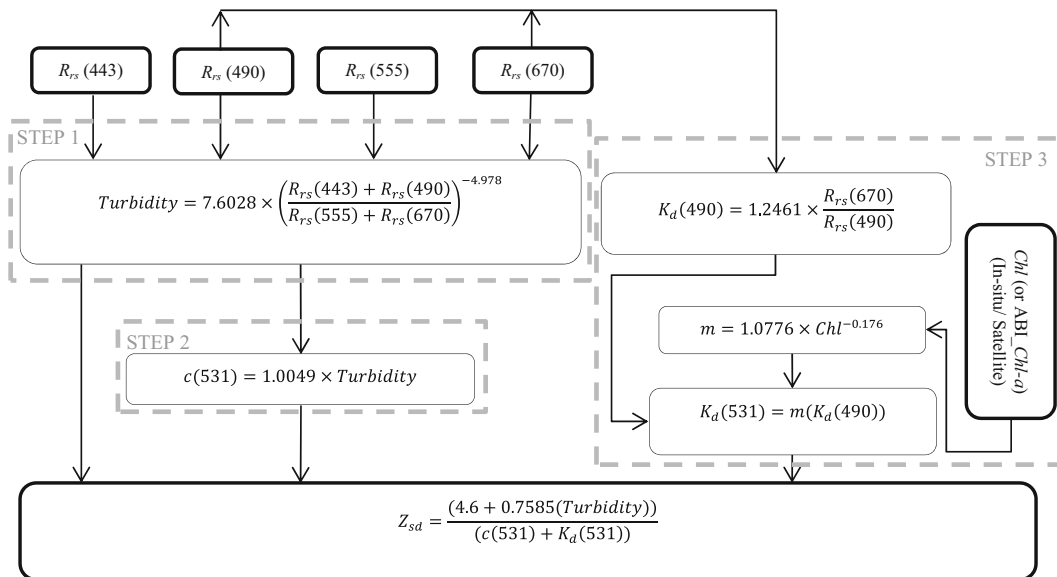


Fig. 2 Flowchart showing the steps involved in estimating the underwater vertical visibility parameter (Z_{sd}) from remote sensing data

concentration of chlorophyll is important in predicting the variation in spectral magnitude of K_d in the blue-green domain in turbid coastal and inland waters. The validation exercise (using in situ data $N = 61$) indicated that the modeled $K_d(531)$ had significantly low errors ($RMSE = 0.06$) and high correlation coefficient ($R^2 = 0.94$) (Fig. 5c). Moreover, a scatterplot for $K_d(531)$ was also plotted using the NOMAD data set which showed the one-to-one correspondence between modeled and in situ $K_d(531)$ (Fig. 5d). A careful investigation carried out to obtain the optical relationship between the measured chlorophyll concentration and the TSS revealed a highly unsystematic pattern of the data points for all the sampling stations. Therefore, it can be implied that no correlation existed between these two parameters in coastal waters under investigation.

Application to in situ and remote sensing data The present algorithm was applied to MODIS-Aqua images to estimate the Z_{sd} parameter in coastal waters off Point Calimere and Chennai along the Tamil Nadu coast. The MODIS image covered the scene extending from Chennai to the southernmost tip of India (Kanyakumari). The Z_{sd} transparency was mapped typically ranging from 0 to a maximum of 25 m which revealed that the predicted Z_{sd} increases from shallow turbid waters to deep clear waters in the coastal regions of the Bay of Bengal (Fig. 6a–f).

The performance of the present algorithm was further examined by comparing the Z_{sd} contour plots (measured, modeled, and satellite-derived Z_{sd}) for the month of January 2014 and August 2013. To obtain the contour maps, Z_{sd} at known latitudes and

Fig. 3 **a** Relationship between turbidity and Rrs band ratio $(Rrs(443) + Rrs(490)) / (Rrs(555) + Rrs(670))$ from the Indian in situ data set ($N = 59$). **b** Scatterplot showing the one-to-one correlation between measured and modeled turbidity (NTU) ($N = 32$)

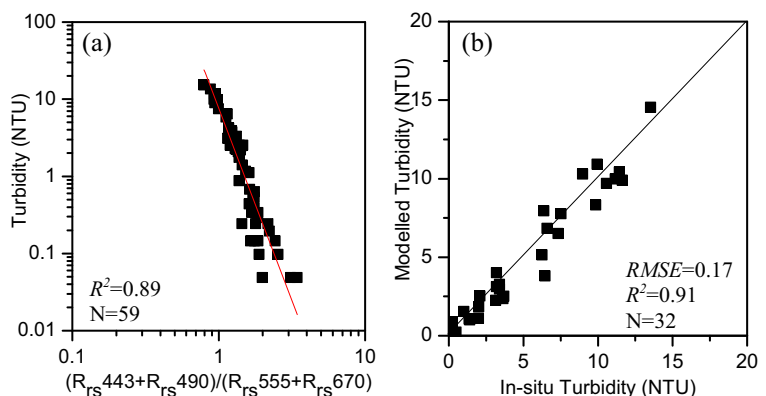
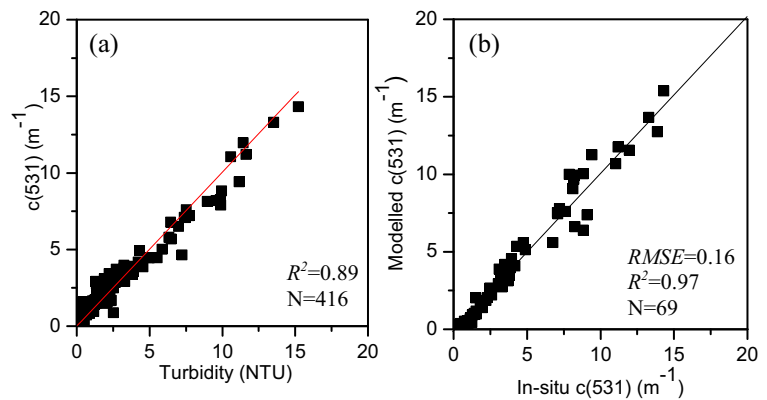


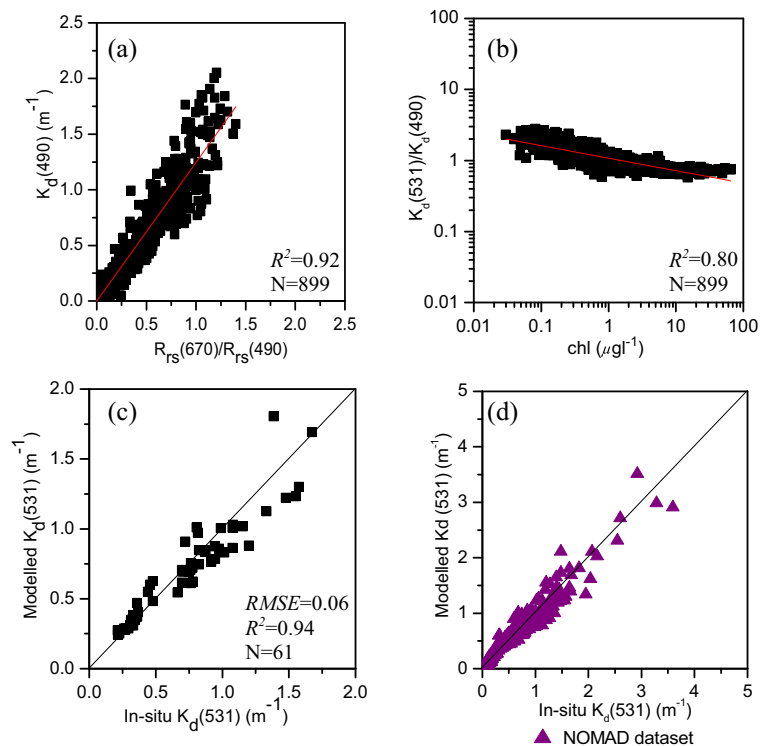
Fig. 4 **a** Relationship between beam attenuation coefficient, $c(531)$, and turbidity from Indian ($N = 416$) data set. **b** Comparison of modeled $c(531)$ with in situ $c(531)$ ($N = 69$)



longitudes from the sampling points was used and the inverse distance weightage (IDW) technique was adopted to generate the contour plots. This technique uses the inverse to power the gridding method to visualize the pattern of Z_{sd} with better interpretation. The generated grid of contour plots indicated that the modeled and MODIS-Aqua-derived Z_{sd} closely matched with the measured (in situ) contour maps (Fig. 7). The contour plots for measured Z_{sd} were generated based on the spatial variation of observed in situ Z_{sd} data points. With a view to capture and examine the spatial variation more effectively, the

data points which well distribute over the entire grid area (colored region) were selected to obtain the contour patterns. Such even distribution of data points minimized the discrepancy in the contour pattern which might have been caused due to uneven spread of data points in the grid. The corresponding contour plots generated for modeled and satellite-derived Z_{sd} showed a close resemblance with contour patterns of the measured Z_{sd} which further confirms the even distribution of the data points over the entire grid locations. The data points were uniformly spread across the contour maps generated.

Fig. 5 **a** Relationship between $K_d(490)$ and band ratio $R_{rs}(670)/R_{rs}(490)$ from NOMAD ($N = 827$) and Indian ($N = 72$) data sets. **b** Power relationship between $Chl-a$ ($\mu g l^{-1}$) and $K_d(531)/K_d(490)$ to obtain $K_d(531)$ ($N = 899$). **c** Scatterplot showing the one-to-one correlation between measured and modeled $K_d(531)$ obtained for Indian in situ data set ($N = 61$). **d** Scatterplot showing one-to-one correspondence for $K_d(531)$ using NOMAD



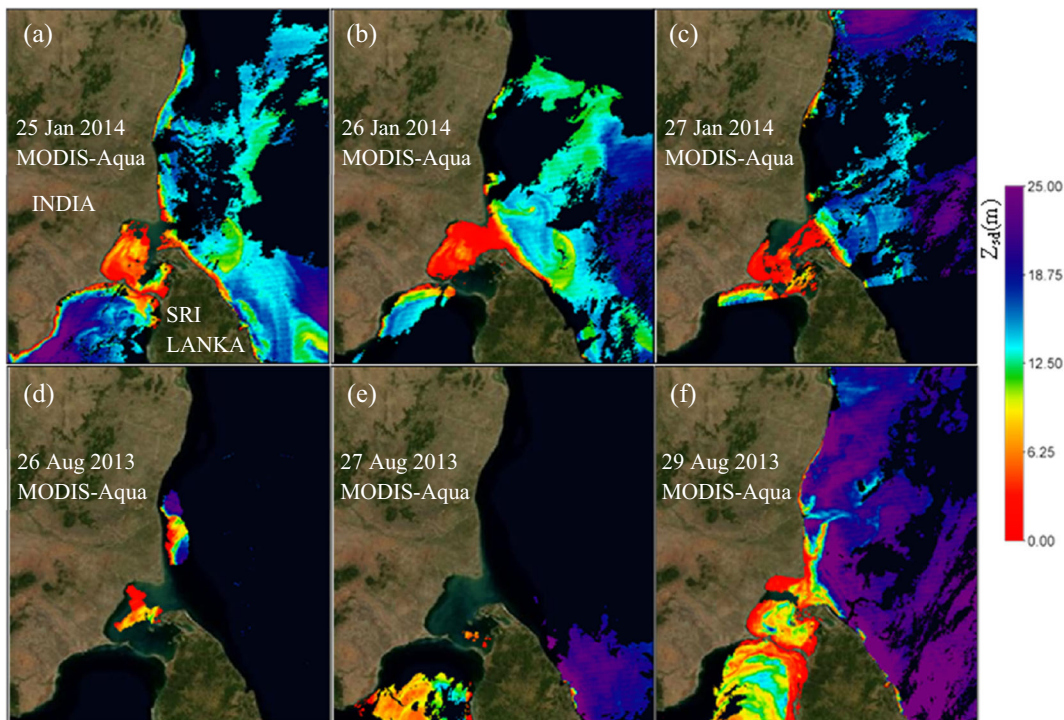


Fig. 6 The water transparency map depicting the remotely derived Z_{sd} using the present algorithm. **a–f** MODIS-Aqua imagery covering the coastal region of Point Calimere and deep waters of Bay of Bengal

Comparative study Several algorithms have been applied to remote sensing data for estimating the water transparency in coastal and inland waters (Giardino et al. 2001; Zhang et al. 2003; Suresh et al. 2006; Stock 2015; Chen et al. 2007b). However, such algorithms do not reveal the method to predict the value of the coupling coefficient, thereby ignoring the contrast transmittance theory despite its importance in estimating the underwater visibility (Tyler 1968; Preisendorfer 1986; Davies-Colley 1988; Doron et al. 2007; Hou et al. 2007). One such existing standard algorithm (Suresh et al. 2006) has been included in the present study with a view to demonstrate its performance in terms of statistical measures. The algorithm comprises an empirical relationship which was derived using the radiometric data for a region of the Arabian Sea and is simply expressed by

$$Z_{sd} = 2.27212 + 7.239 \left(\frac{R_{rs}(490)}{R_{rs}(555)} \right) \quad (24)$$

The modeled and satellite-derived Z_{sd} values were evaluated for the Suresh et al. (2006) algorithm and the present algorithm. These Z_{sd} values estimated for

the independent in situ data and satellite data and compared with those of the observations. For the present algorithm, the Z_{sd} values estimated for the independent in situ data showed significantly low errors and high slope and R^2 values ($MRE = -0.020$, $RMSE = 0.075$, slope = 0.94, intercept = 0.03, bias = 0.009, $R^2 = 0.95$, $N = 38$). The MODIS-Aqua-derived Z_{sd} yielded $MRE = -0.016$, $RMSE = 0.079$, bias = 0.06, slope = 0.93, intercept = 0.05, and $R^2 = 0.95$ for $N = 23$ (shown in Table 1 (a)). For the algorithm by Suresh et al. (2006), Z_{sd} yielded an $RMSE = 0.6263$, $MRE = 1.22$, bias = -0.536 , slope = 6.37, intercept = -5.77 , and $R^2 = 0.80$ ($N = 38$). For the satellite matchup data, it yielded $RMSE = 0.517$, $MRE = 0.7$, bias = -0.413 , slope = 5.61, intercept = -5.02 , and $R^2 = 0.744$ ($N = 23$) (Table 1 (b)). Furthermore, the independent validation was carried out for the modeled and the satellite-derived Z_{sd} values which included a total of 38 and 23 data points, respectively. The corresponding one-to-one scatterplots of modeled and satellite-derived Z_{sd} versus measured Z_{sd} demonstrate the robustness of the present algorithm in predicting Z_{sd} in both turbid and clear waters (Fig. 8a, b).

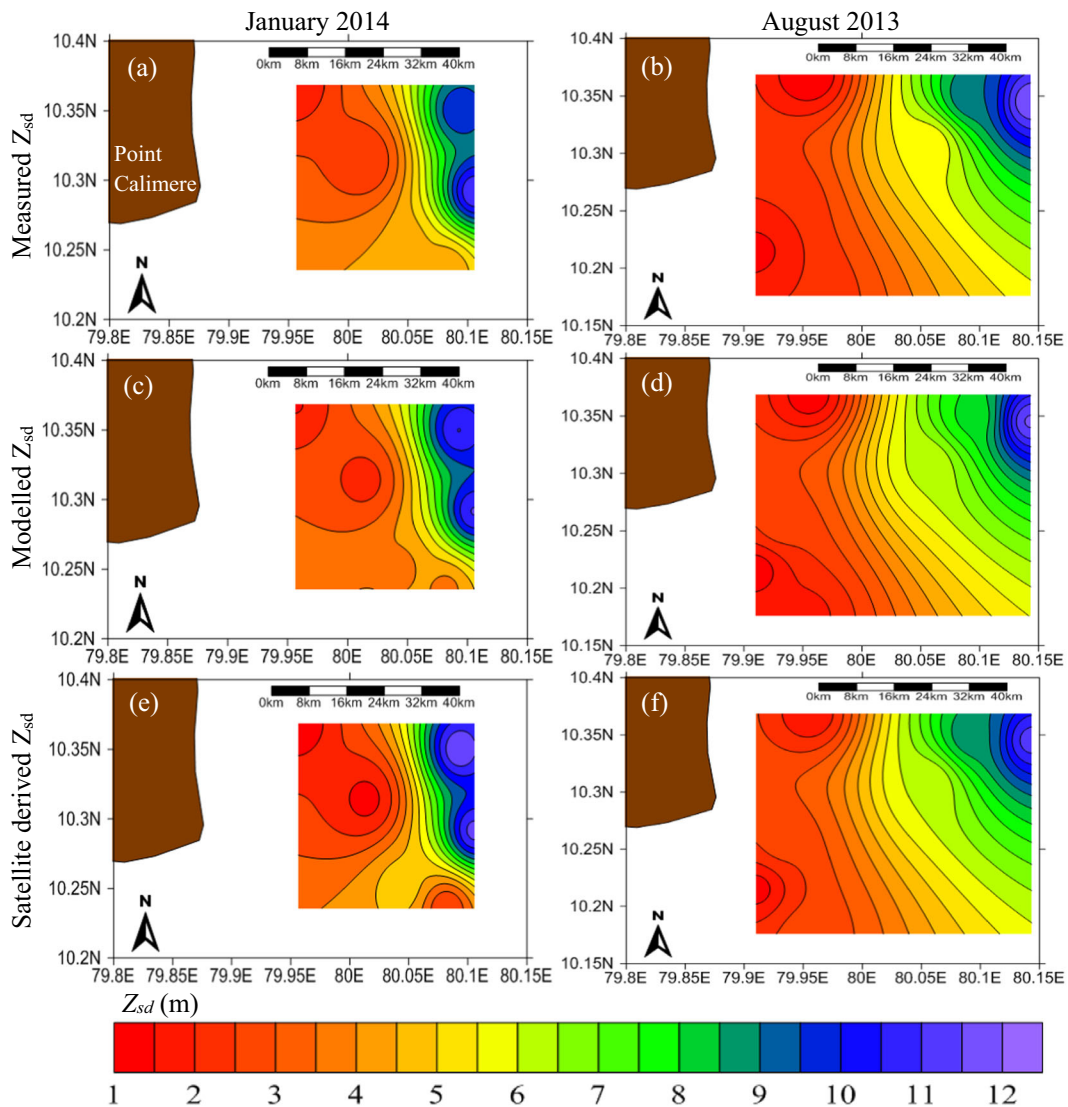


Fig. 7 Comparison of contour plots for the measured, modeled, and MODIS-Aqua-derived Z_{sd} in coastal waters off Point Calimere

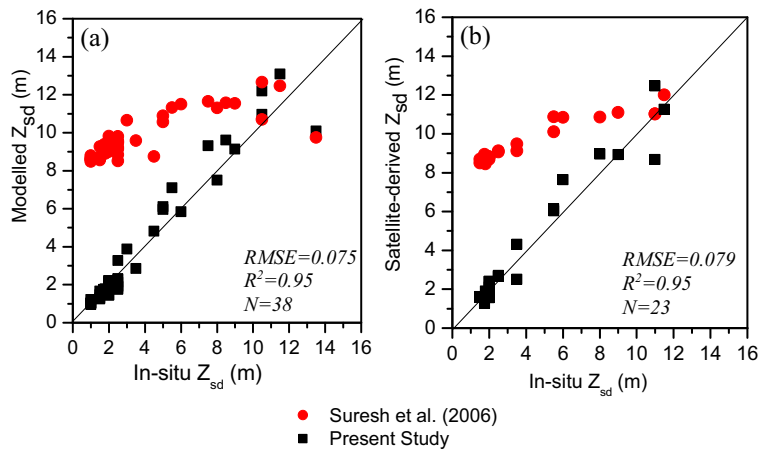
It was found that the model proposed by Suresh et al. (2006) provides higher *RMSE* and *MRE* values in complex coastal waters, when compared with the present

algorithm (Fig. 8a, b). The 38 and 23 matchups for the modeled and the satellite-derived Z_{sd} values were used for both the present study and that of Suresh et al.

Table 1 Error statistics to evaluate the performance of modeled and satellite-derived Z_{sd}

	<i>RMSE</i>	<i>MRE</i>	Bias	Slope	Intercept	R^2	<i>N</i>
(a) Present study							
Z_{sd} (in situ validation)	0.075	-0.020	0.009	0.94	0.03	0.95	38
Z_{sd} (satellite matchup validation)	0.079	-0.016	0.006	0.93	0.05	0.95	23
(b) Suresh et al. (2006)							
Z_{sd} (in situ validation)	0.626	1.22	-0.536	6.37	-5.77	0.80	38
Z_{sd} (satellite matchup validation)	0.517	0.70	-0.413	5.61	-5.02	0.74	23

Fig. 8 Scatterplot for Suresh et al. (2006) and present study showing the comparison between **a** modeled and in situ measured Z_{sd} ($N = 38$) and **b** satellite-derived Z_{sd} and in situ measured Z_{sd} ($N = 23$)



(2006), and the corresponding statistical values are provided in Table 1. The improved statistical values for the present algorithm further demonstrate that the satellite-derived Z_{sd} can be accurately estimated through the proper addressal of the coupling coefficient without deviating from the contrast transmittance theory. It can be further implied that the principle of ocean color remote sensing when coupled with the contrast transmittance theory plays a crucial role and can overcome the major limitation of existing algorithms in complex coastal waters.

Discussion

The present study reveals that the integral components of the algorithm developed to derive the satellite-based Z_{sd} can be obtained through the careful selection of band ratios of R_{rs} in the visible spectrum. Besides, the band ratio of R_{rs} contains crucial information related to optical properties of the water column. These optical properties are of prime importance in predicting the behavior of the underwater light field and, hence, the variation in water transparency parameter under various illumination conditions.

The coupling coefficient has been determined by means of turbidity using the band ratio technique. The band ratio is employed to determine Z_{sd} based on the fact that the reflectance ratio is less susceptible to ambiguities in the atmospheric correction scheme than the absolute values of reflectance. In the present study, a four-band algorithm has been developed that employs R_{rs} at 443, 490, 555, and 670 nm yielding the best fit

through regression analysis on the data set for a wide range of water types within the study region. c essentially follows a linear relationship with turbidity, and the slope is optimized to achieve increased accuracy for the satellite-derived Z_{sd} for both turbid and clear waters. The proposed four-band algorithm suggests that the light reflected in the visible wavelengths highly correlates to proxy of TSS concentration expressed in terms of turbidity. The band ratio also takes into account the influence of two vital absorption bands of chlorophyll which are centered at 443 and 670 nm. Thus, the turbidity algorithm performs well in turbid coastal and turbid productive inland waters as well as relatively clear offshore waters, where standard red and near-infrared (NIR) band ratio-based algorithms tend to fail owing to their adaptation only in turbid waters.

The variation of slope in the blue-green region of the K_d spectra, owing to the contribution of chlorophyll concentration, is well understood from the mathematical power function. The magnitude of the chlorophyll concentration governs the variation in the spectral slope of $K_d(531)$ to $K_d(490)$. Thus, the spectral band ratio of K_d has been chosen allowing that it captures the physical effect of chlorophyll and positively correlates to $K_d(531)$. Furthermore, it becomes imperative to incorporate an effective algorithm to estimate the surface chlorophyll concentration if one has to retrieve Z_{sd} from satellite data in turbid coastal waters. The two-step algorithm applied to determine $K_d(531)$ has potentially enhanced our understanding in the aspect that the magnitude of chlorophyll concentration clearly influences the spectral behavior (relative change in slope) of K_d at the shorter wavelength region, which cannot be overlooked. Furthermore, it can also be implied with

confidence that the correlation between the K_d and R_{rs} band ratio can be of paramount importance in predicting the bio-optical state of various oceanic waters, provided an effective and appropriate atmospheric correction scheme has been accounted for such applications. In the present study, the ABI *Chl-a* algorithm was used based on the fact that retrieved *Chl-a* gave a similar trend of correlation with the in situ data. This *Chl-a* parameter is closely correlated to $K_d(531)$ based on a power-law relationship as demonstrated by Eq. (22). Thus, the derived *Chl-a* has an important implication in estimating Z_{sd} in inland and marine waters.

The present study demonstrates the bio-optical correlation, between the chlorophyll concentration and the slope of $K_d(490)$ to $K_d(531)$, which can be used to predict $K_{d,PAR}$ for remote sensing of the primary productivity. The value of K_d when calculated in the photosynthetically active radiation (PAR) over the visible waveband region at any depth (z) is known as $K_{d,PAR}$ (m^{-1}). $K_{d,PAR}$ (m^{-1}) is calculated by computing the integral of the $E_d(\lambda, z)$ spectrum in the entire visible domain ranging from 400 to 700 nm (Tyler 1966; Saulquin et al. 2013). However, $K_{d,PAR}$ can also be retrieved using $K_d(531)$ as the key input optical parameter based on the fact that the $K_{d,PAR}$ bears a positive correlation with K_d in the green portion of the visible spectrum, where the attenuation is minimum, as reported in the study by Gallegos (2001). The derived $K_{d,PAR}$ can be further investigated to predict the pattern of primary productivity (either regionally or globally) or trophic status over the spatio-temporal scales for lakes and inland waters (Platt and Satyendranath 1988; Sakshaug et al. 1997; Mélin and Hoepffner 2011). The product of Z_{sd} and $K_{d,PAR}$ can be used as a crucial parameter to determine the index of water quality which is mathematically expressed as $K_{d,PAR} \times Z_{sd}$. This mathematical identity has significant implications in classifying the optically different classes of lakes and identifying the conditions of low level of transparency in turbid lakes and coastal waters (Reinart et al. 2003; Ma et al. 2016).

The *TSI* is a highly desired parameter to identify the trophic status of lakes and coastal waters and provide a standard scale for classification of marine ecosystems characterized with low eutrophic (ultra-oligotrophic) or extremely high eutrophic (hyper-eutrophic) conditions. Such predictive scaling tool can be developed based on the inter-relationships of Z_{sd} with algal biomass and nutrient (such as total phosphorus) concentration or

loading, which are identified as major factors of eutrophication in coastal and inland waters (Carlson 1977; Baban 1996; Cheng and Lei 2001).

The present study was carried out for two main seasons, namely, southwest monsoon (June to September) and northeast monsoon (October to January), which chiefly dominate the oceanography of Bay of Bengal, to investigate the seasonal variability in Z_{sd} and thereby understand the role of coastal dynamic processes in water transparency. The Z_{sd} map for MODIS imagery in the month of January 2014 reveals lower transparency when compared to August 2013. The difference in Z_{sd} observed may be attributed to the tropical storms that occur frequently during the northeast monsoon period in the Bay of Bengal. The tropical storms and cyclones induce a surface drift along the east coast, thereby resulting in greater longshore sediment transport in the southerly direction. The extreme wave conditions accrued during the episodic cyclonic events tend to remove the sediment from coastline whereby increasing its concentration in the most vulnerable areas which are highly sensitive to siltation. In such conditions, reduced light penetration in the water column can be expected, which is well demonstrated in the MODIS imagery for the month of January (shown in Fig. 6a–f). Furthermore, it can be clearly seen that the area northeast of the Gulf of Mannar (i.e., Palk Bay seen as red patch) takes most of the sediment load and is under heavy siltation throughout the year.

It can be inferred that a large variation in the seasonal currents and sediment runoff greatly affects the water transparency along the east coast of India between pre-monsoon and post-monsoon periods. The high sedimentation near the coast, as observed in the MODIS images, occurs due to the entrapment of fluvial discharge and re-suspended sediments into the coastal waters, which reduces offshore sediment influx in deeper regions of the Bay of Bengal. Thus, water transparency is higher in the open seas than in the coastal zone for both the seasons (Sanil Kumar et al. 2006; Deo and Ganer 2014).

The pattern of Z_{sd} obtained from MODIS-Aqua data further confirms the wider applicability of the present algorithm in estimating the Z_{sd} on different spatio-temporal scales. The spatial contours have been included to provide the best data visualization of the measured, modeled, and satellite-based Z_{sd} . The one-to-one correspondence achieved between measured, modeled, and satellite-derived Z_{sd} well

establishes the significant role of the contrast transmittance theory and coupling coefficient in closely predicting the Z_{sd} for complex water types.

Conclusion

A new methodology has been presented to estimate Z_{sd} from satellite data in turbid and clear waters. This approach adopts the key concept of coupling the remote sensing technique within the framework of the contrast transmittance theory. The present Z_{sd} algorithm closely determined the coupling coefficient and addressed its variable nature in various water types (clear and turbid coastal waters), as it follows the contrast transmittance theory unlike the existing algorithms. The proposed algorithm is a simple and effective tool to predict Z_{sd} based on the coupling coefficient and integral components of the contrast transmittance theory. The coupling coefficient is expressed as the function of turbidity which can be easily derived from the R_{rs} data. Since turbidity, c , and K_d are the input parameters to estimate Z_{sd} , the accuracy of the functional relationships for predicting these intermediate parameters was ensured by the validation analyses. The error associated with Z_{sd} estimates in estuarine and coastal regions showed an *MRE* and *RMSE* within ± 25 and 10%, respectively, for the modeled and the satellite-derived Z_{sd} .

The present algorithm also incorporates an accurate case 2 water bio-optical algorithm (ABI *Chl-a* algorithm) to obtain the chlorophyll concentration in turbid coastal waters to avoid such deviations. Furthermore, in spite of the large variation in optical properties of coastal waters of Point Calimere and Chennai in the Bay of Bengal, an accurate estimation of turbidity and Z_{sd} was achieved.

The present algorithm also outperformed the Suresh et al. (2006) algorithm (which is simply a function of the R_{rs} ratio without involving the contrast transmittance theory) in terms of estimating the Z_{sd} with much higher accuracy. The proposed algorithm was further applied to several MODIS-Aqua, and subsequently, matchup comparisons were performed for validating the derived products. The results showed that Z_{sd} can be accurately derived based on the coupled concepts of remote sensing and the contrast transmittance theory, unlike other standard existing algorithms that rely mainly on the conventional band ratio techniques involving direct relationships between R_{rs} and Z_{sd} .

The present model can be useful in understanding the coastal processes and sediment transport—which are crucial for coastal management and protection works. With the primary information about sedimentation process, remedial measures can be adopted in adverse cases such as siltation of harbors, accumulation of sand bars which might accrue navigational hazards, or degradation of coastal environment. The exposure of sediment (concentration and duration) either suspended or bed loaded largely determines the distribution of SAV and controls the biological response of fish, marine species, shellfish, and aquatic plants. The information about the degree of light penetration would also aid in assessing the concentration and distribution of CDOM, which essentially affect the distribution of SAV (Chen et al. 2015). Z_{sd} has been recognized as a proxy of visual water clarity and forms a major link-pin to assess the trophic index of inland water bodies (Cialdi and Secchi 1865; Collier et al. 1968; Tyler 1968; Carlson 1977; Trees et al. 2005; Fleming-Lehtinen and Laamanen 2012). A large data base of water clarity information based on Secchi disk transparency is vital to water quality managers as it assists them to design better strategies for developing recreational resources in the coastal zone and making tourism management decisions economically effective (Wetzel and Likens 1979; Effler 1988). The change in the water clarity can be well correlated (either empirically or semi-empirically) to variation in phytoplankton abundance. Such predictions have significant implications in management activities where control on algal growth is seen as an effective strategy to monitor water quality (DFAS 2001; Hoyer et al. 2014). Thus, the estimation of Secchi disk transparency helps limnologists and water quality managers to design a better strategy for monitoring water quality and water management activities in coastal and estuarine waters (Effler 1988; Chen et al. 2007b). The assessment of water clarity can provide an insight into the distribution and type of benthic organisms (such as fishes or corals) and the productivity rate of phytoplankton (micro-organisms) as their ecological behavior and response very much depend on the degree of light available in the aquatic environment. Therefore, it can be implied that the estimation of water transparency on various spatio-temporal scales aids to understand the ecological behavior of aquatic organisms (benthic organisms) and their response to dynamic environment (Weeks et al. 2012). The Z_{sd} parameter provides the indirect way to measure the biological productivity of

an aquatic system. Therefore, Secchi transparency information is useful in monitoring water quality from the perspective of the biological productivity of a water body. Furthermore, the assessment of water clarity can be crucial in enhancing our knowledge on phytoplankton abundance, dissolved substance, or associated trophic state caused due to nutrient loading in inland and coastal water environments. Such information can be well leveraged to adopt appropriate measures to manage water clarity activities (DFAS 2001).

The water transparency can be used as a crucial linking parameter to assess the level of eutrophication in near-shore and inland waters which largely influences the ecological functioning of these waters (Tapia González et al. 2008). The method proposed in the present study to derive satellite-based Z_{sd} can be adopted as a crucial preliminary step to retrieve the satellite-based trophic index of eutrophic water bodies. The estimation of water transparency over spatial and temporal scales would also be useful in understanding and evaluating the near- or far-term impacts of coastal land usage on marine environment (Ucuncuoglu et al. 2006). Thus, the proposed method will serve as an important tool in monitoring of the aquatic ecosystem and water quality conditions within coastal and near-shore environments.

Acknowledgements This research was supported by the Department of Science and Technology (OEC/16-17/130/DSTX/PSHA) under the HSRS program and the Indian Institute of Technology Madras through the MHRD fellowship. We would like to extend our thanks to D. Rajshekhar, The Head, Vessel Management Cell (VMC), and the Director of National Institute of Ocean Technology (NIOT), for providing the Coastal research vessels (CRV Sagar Paschimi and CRV Sagar Purvi) to IIT Madras for carrying out various underwater light field measurements during the cruises and developing the bio-optical models. We gratefully acknowledge the contributors and scientists who contributed to NOMAD and the Ocean Biology Processing Group of NASA for the distribution of the NOMAD in situ data and the support of the SeaDAS 7.2 Software. We sincerely thank the two anonymous reviewers for their valuable comments and suggestions to improve the manuscript.

References

- Akbar, T. A., Hassan, Q. K., & Achari, G. (2014). Development of remote sensing based models for surface water quality. *Clean - Soil, Air, Water*, 42(8), 1044–1051. doi:10.1002/clean.201300001.
- Baban, S. M. (1996). Trophic classification and ecosystem checking of lakes using remotely sensed information. *Hydrological Sciences Journal*, 41(6), 939–957.
- Balali, S., Hoseini, S. A., Ghorbani, R., & Balali, S. (2013). Correlation of chlorophyll-a with Secchi disk depth and water turbidity in the International Alma Gol Wetland, Iran. *Middle-East Journal Scientific Research*, 13(10), 1296–1301. doi:10.5829/idosi.mejsr.2013.13.10.1124.
- Berkman, J.A.H., & Canova, M.G. (2007). Algal biomass indicators. In: Myers, D.N., and Sylvester, M.D., *National field manual for the collection of water-quality data-Biological indicators: US Geological Survey Techniques of Water-Resources Investigations, book 9*. US Geological Survey TWRI, ABI1-ABI86.
- Berwald, J., Stramski, D., Mobley, C. D., & Kiefer, D. A. (1998). Effect of Raman scattering on the average cosine and diffuse attenuation coefficient of irradiance in the ocean. *Limnology and Oceanography*, 43(4), 564–576. doi:10.4319/lo.1998.43.4.0564.
- Carlson, R. E. (1977). A trophic state index for lakes. *Limnology and Oceanography*, 22(2), 361–369. doi:10.4319/lo.1977.22.2.0361.
- Chauhan, O. S., Rajawat, A. S., Pradhan, Y., Suneethi, J., & Nayak, S. R. (2005). Weekly observations on dispersal and sink pathways of the terrigenous flux of the Ganga-Brahmaputra in the Bay of Bengal during NE monsoon. *Deep Sea Research Part II: Topical Studies in Oceanography*, 52(14–15), 2018–2030. doi:10.1016/j.dsr2.2005.05.012.
- Chen, Z., Doering, P. H., Ashton, M., & Orlando, B. A. (2015). Mixing behavior of colored dissolved organic matter and its potential ecological implication in the Caloosahatchee River Estuary, Florida. *Estuaries and Coasts*, 38(5), 1706–1718. doi:10.1007/s12237-014-9916-0.
- Chen, Z., Hu, C., & Muller-Karger, F. (2007a). Monitoring turbidity in Tampa Bay using MODIS/Aqua 250-m imagery. *Remote Sensing of Environment*, 109(2), 207–220. doi:10.1016/j.rse.2006.12.019.
- Chen, Z., Muller-karger, F. E., & Hu, C. (2007b). Remote sensing of water clarity in Tampa Bay. *Remote Sensing of Environment*, 109(2), 249–259. doi:10.1016/j.rse.2007.01.002.
- Cheng, K. S., & Lei, T. C. (2001). Reservoir trophic state evaluation using Lanisat TM images. *JAWRA Journal of the American Water Resources Association*, 37(5), 1321–1334.
- Cialdi, M., & Secchi, P. A. (1865). Sur la transparence de la mer. *Comptes Rendus de l'Académie des Sciences*, 61.
- Collier, A., Finlayson, G. M., & Cake, E. W. (1968). On the transparency of the sea: observations made by Mr. Ciladi and P.A. Secchi. *Limnology and Oceanography*, 13, 391–394.
- Davies-Colley, R. J. (1988). Measuring water clarity with a black disk. *Limnology and Oceanography*, 33(4 part 1), 616–623. doi:10.4319/lo.1988.33.4.0616.
- Deo, A. A., & Ganer, D. W. (2014). *Tropical cyclone activity over the Indian Ocean in the warmer climate: monitoring and prediction of tropical cyclones in the Indian Ocean and climate change* (pp. 72–80). Dordrecht: Springer. doi:10.1007/978-94-007-7720-0_7.
- DFAS (2001). Florida LAKEWATCH: a beginner's guide to water management—water clarity, Information Circular 103,

- Department of Fisheries and Aquatic Sciences, Institute of Food and Agricultural Sciences, University of Florida, 3rd Edition.
- Doron, M., Babin, M., Mangin, A., & Hembise, O. (2007). Estimation of light penetration, and horizontal and vertical visibility in oceanic and coastal waters from surface reflectance. *Journal of Geophysical Research*, *112*(C6), C06003. doi:10.1029/2006JC004007.
- Effler, S. W. (1988). Secchi disc transparency and turbidity. *Journal of Environmental Engineering*, *114*(6), 1436–1447.
- Ellison, C. A., Kiesling, R. L., & Fallon, J. D. (2010). *Correlating streamflow, turbidity, and suspended-sediment concentration in Minnesota's Wild Rice River. 2nd Joint Federal Interagency Conference* (p. 10). Las Vegas.
- Fleming-Lehtinen, V., & Laamanen, M. (2012). Long-term changes in Secchi depth and the role of phytoplankton in explaining light attenuation in the Baltic Sea. *Estuarine, Coastal and Shelf Science*, *102*, 1–10.
- Gallegos, C. L. (2001). Calculating optical water quality targets to restore and protect submersed aquatic vegetation: overcoming problems in partitioning the diffuse attenuation coefficient for photosynthetically active radiation. *Estuaries*, *24*(3), 381–397.
- Giardino, C., Pepe, M., Brivio, P. A., Ghezzi, P., & Zilioli, E. (2001). Detecting chlorophyll, Secchi disk depth and surface temperature in a sub-alpine lake using Landsat imagery. *Science of the Total Environment*, *268*(1–3), 19–29. doi:10.1016/S0048-9697(00)00692-6.
- Holmes, R. W. (1970). The Secchi disk in turbid coastal waters. *Limnology and Oceanography*, *15*(5), 688–694. doi:10.4319/lo.1970.15.5.0688.
- Hou, W., Lee, Z., & Weidemann, A. D. (2007). Why does the Secchi disk disappear? An imaging perspective. *Optics Express*, *15*(6), 2791–2802.
- Hoyer, M. V., Bigham, D. L., Bachmann, R. W., & Canfield Jr., D. E. (2014). Florida LAKEWATCH: citizen scientists protecting Florida's aquatic systems. *Florida Scientist*, *77*(4), 184.
- Kulshreshtha, A., & Shanmugam, P. (2015). An optical method to assess water clarity in coastal waters. *Environmental Monitoring and Assessment*, *187*(12), 742. doi:10.1007/s10661-015-4953-0.
- Lee, Z., Shang, S., Hu, C., Du, K., Weidemann, A., Hou, W., Lin, J., & Lin, G. (2015). Secchi disk depth: a new theory and mechanistic model for underwater visibility. *Remote Sensing of Environment*, *169*(2015), 139–149. doi:10.1016/j.rse.2015.08.002.
- Levin, I., Darecki, M., Sagan, S., & Radomyslskaya, T. (2013). Relationships between inherent optical properties in the Baltic Sea for application to the underwater imaging problem. *Oceanologia*, *55*(1), 11–26. doi:10.5697/oc.55-1.011.
- Ma, J., Song, K., Wen, Z., Zhao, Y., Shang, Y., Fang, C., & Du, J. (2016). Spatial distribution of diffuse attenuation of photosynthetic active radiation and its main regulating factors in inland waters of Northeast China. *Remote Sensing*, *8*(11), 964.
- Mélin, F., & Hoepffner, N. (2011). Monitoring phytoplankton productivity from satellite—an aid to marine resources management. Handbook of satellite remote sensing image interpretation: applications for marine living resources conservation and management, edited by: Morales, J., Stuart, V., Platt, T., and Sathyendranath, S., *EU PRESPO and IOCCG*, 79–93.
- Mobley, C. D. (1999). Estimation of the remote-sensing reflectance from above-surface measurements. *Applied Optics*, *38*(36), 7442–7455. doi:10.1364/AO.38.007442.
- Moreno, J.P. (2013). Evaluation of Secchi depth of remote sensing techniques in Deer Creek Reservoir, Utah. *M.S Thesis, Department of Civil and Environmental Engineering, Brigham Young University*, pp 52.
- Nasiha, H. J., & Shanmugam, P. (2015). Estimating the bulk refractive index and related particulate properties of natural waters from remote-sensing data. *IEEE Journal of Selected Topics In Applied Earth Observations and Remote Sensing*, *8*(11), 5324–5335. doi:10.1109/jstars.2015.2439581.
- Ohde, T., & Siegel, H. (2003). Derivation of immersion factors for the hyperspectral TriOS radiance sensor. *Journal of Optics A: Pure and Applied Optics*, *5*(2003), L12–L14.
- Ouillon, S., Douillet, P., Petrenko, A., Neveux, J., Dupouy, C., Froidefond, J.-M., Andréfouët, S., & Muñoz-Caravaca, A. (2008). Optical algorithms at satellite wavelengths for total suspended matter in tropical coastal waters. *Sensors*, *8*(7), 4165–4185. doi:10.3390/s8074165.
- Pegau, W. S., Gray, D., & Zaneveld, J. R. V. (1997). Absorption and attenuation of visible and near-infrared light in water: dependence on temperature and salinity. *Applied Optics*, *36*(24), 6035–6046. doi:10.1364/ao.36.006035.
- Pegau, W. S., & Zaneveld, J. R. V. (1993). Temperature-dependent absorption of water in the red and near-infrared portions of the spectrum. *Limnology and Oceanography*, *38*(1), 188–192. doi:10.4319/lo.1993.38.1.0188.
- Platt, T., & Sathyendranath, S. (1988). Oceanic primary production: estimation by remote sensing at local and regional scales. *Science*, *241*, 1613–1620.
- Pope, R. M., & Fry, E. S. (1997). Absorption spectrum (380–700 nm) of pure water. II. Integrating cavity measurements. *Applied Optics*, *36*(33), 8710–8723.
- Preisendorfer, R. W. (1986). Secchi disk science: visual optics of natural waters. *Limnology and Oceanography*, *3*(5), 909–926. doi:10.4319/lo.1986.31.5.0909.
- Reinart, A., Herlevi, A., Arst, H., & Sipelgas, L. (2003). Preliminary optical classification of lakes and coastal waters in Estonia and south Finland. *Journal of Sea Research*, *49*(4), 357–366.
- Sakshaug, E., Bricaud, A., Dandonneau, Y., Falkowski, P. G., Kiefer, D. A., Legendre, L., Morel, A., Parslow, J., & Takahashi, M. (1997). Parameters of photosynthesis: definitions, theory and interpretation of results. *Journal of Plankton Research*, *19*(11), 1637–1670.
- Sanil Kumar, V., Pathak, K. C., Pednekar, P., Raju, N. S. N., & Gowthaman, R. (2006). Coastal processes along the Indian coastline. *Current Science*, *91*(4), 530–536.
- Saulquin, B., Hamdi, A., Gohin, F., Populus, J., Mangin, A., & d'Andon, O. F. (2013). Estimation of the diffuse attenuation coefficient KdPAR using MERIS and application to seabed habitat mapping. *Remote Sensing of Environment*, *128*, 224–233.
- Selvaraj, K., Mohan, V. R., Jonathan, M. P., & Srinivasalu, S. (2005). Modification of a coastal environment: Vedaranniyam wetland, southeast coast of India. *Journal of the Geological Society of India*, *66*(5), 535–538.

- Shanmugam, P. (2011). A new bio - optical algorithm for the remote sensing of algal blooms in complex ocean waters. *Journal of Geophysical Research*, 116(C4), 1–12. doi:10.1029/2010JC006796.
- Siegel, D.A., & Dickey, T.D. (1988). Characterization of downwelling spectral irradiance fluctuations. *Proceedings of the 9th Conference of Ocean Optics*. (Orlando, FL, USA, SPIE), pp. 67–74.
- Simon, A., & Shanmugam, P. (2013). A new model for the vertical spectral diffuse attenuation coefficient of downwelling irradiance in turbid coastal waters: validation with in situ measurements. *Optics Express*, 21(24), 30082–30106. doi:10.1364/oe.21.030082.
- Simon, A., & Shanmugam, P. (2016). Estimation of the spectral diffuse attenuation coefficient of downwelling irradiance in inland and coastal waters from hyperspectral remote sensing data: Validation with experimental data. *International Journal of Applied Earth Observation and Geoinformation*, 49(2016), 117–125. doi:10.1016/j.jag.2016.02.003.
- Singh, R. K., & Shanmugam, P. (2014). A novel method for estimation of aerosol radiance and its extrapolation in the atmospheric correction of satellite data over optically complex oceanic waters. *Remote Sensing of Environment*, 142(2014), 188–206. doi:10.1016/j.rse.2013.12.001.
- Smith, D. G. (2001). A protocol for standardizing Secchi disk measurements, including use of a viewer box. *Lake and Reservoir Management*, 17(2), 90–96.
- Steel, E. A., & Neuhausser, S. (2002). Comparison of methods for measuring visual water clarity. *Journal of North American Benthological Society*, 21(2), 326–335. doi:10.2307/1468419.
- Stock, A. (2015). Satellite mapping of Baltic Sea Secchi depth with multiple regression models. *International Journal of Applied Earth Observation and Geoinformation*, 40(2015), 55–64. doi:10.1016/j.jag.2015.04.002.
- Suresh, T., Naik, P., Bandishte, M., Desa, E., Mascaranahas, A., & Matondkar, S.G.P. (2006). Secchi depth analysis using bio-optical parameters measured in the Arabian Sea. *Asia-Pacific Remote Sensing Symposium, International Society for Optics and Photonics*. pp. 64061Q–64061Q–10. doi:10.1117/12.696251.
- Tapia González, F. U., Herrera-Silveira, J. A., & Aguirre-Macedo, M. L. (2008). Water quality variability and eutrophic trends in karstic tropical coastal lagoons of the Yucatán Peninsula. *Estuarine, Coastal and Shelf Science*, 76(2), 418–430. doi:10.1016/j.ecss.2007.07.025.
- Tiwari, S. P., & Shanmugam, P. (2014). A robust algorithm to determine diffuse attenuation coefficient of downwelling irradiance from satellite data in coastal oceanic waters. *IEEE Journal of Selected Topics in Applied Earth Observations and Remote Sensing*, 7(5), 1616–1622. doi:10.1109/jstars.2013.2282938.
- Trees, C.C., Bissett, P.W., Dierssen, H., Kohler, D.D.R., Moline, M.A., Mueller, J.L., Pieper, R.E., Twardowski, M.S., & Zaneveld, J.R.V. (2005). Monitoring water transparency and diver visibility in ports and harbors using aircraft hyperspectral remote sensing. *Proceedings of Conference of Photonics for Port and Harbor Security*. (Orlando, Florida, USA, SPIE), pp. 91–98. doi:10.1117/12.607554.
- Tyler, J. E. (1966). Report on the the second meeting of the joint group of experts on photosynthetic radiant energy. *UNESCO Technical Papers in Marine Science*, 5, 1–11.
- Tyler, J. E. (1968). The Secchi disc. *Limnology and Oceanography*, 13(1), 1–6. doi:10.4319/lo.1968.13.1.0001.
- Ucuncuoglu, E., Arli, O., & Eronat, A. H. (2006). Evaluating the impact of coastal land uses on water-clarity conditions from Landsat TM/ETM+ imagery: Candarli Bay, Aegean Sea. *International Journal of Remote Sensing*, 27(17), 3627–3643. doi:10.1080/01431160500500326.
- Weeks, S., Werdell, P., Schaffelke, B., Canto, M., Lee, Z., Wilding, J., & Feldman, G. (2012). Satellite-derived photic depth on the great barrier reef: spatio-temporal patterns of water clarity. *Remote Sensing*, 4(12), 3781–3795. doi:10.3390/rs4123781.
- WETLabs. (2010). *Combination fluorometer and turbidity sensor ECO FLNTU user's guide* (p. 28). Philomath, OR: WETLabs Inc..
- Wetzel, R. G., & Likens, G. E. (1979). *Limnological analyses*. Philadelphia, Pa: W. B. Saunders Co..
- Zaneveld, J.R.V., & Kitchen, J.C. (1994). The scattering error correction of reflecting-tube absorption meters. *Proceedings of Ocean Optics XII, International Society for Optics and Photonics*, pp. 44–55.
- Zhang, Y., Pulliainen, J., Koponen, S., & Hallikainen, M. (2003). Empirical algorithms for Secchi disk depth using optical and microwave remote sensing data from the Gulf of Finland and the Archipelago Sea. *Boreal Environment Research*, 8(3), 251–261.